

Semiempirical Investigation of Stilbene-Linked Diradicals and Magnetic Study of Their Bis(*N*-*tert*-butylnitroxide) Variants

Naoki Yoshioka,^{†,§} Paul M. Lahti,^{*,†} Takashi Kaneko,[‡] Yoshihiro Kuzumaki,[‡] Eishun Tsuchida,[‡] and Hiroyuki Nishide^{*,‡}

Department of Chemistry, University of Massachusetts, Amherst, Massachusetts 01003, and Department of Polymer Chemistry, Waseda University, Tokyo 169, Japan

Received January 31, 1994[®]

The electronic states of open-shell stilbene diradicals were studied. Previously used semiempirical MO-CI methods were applied to stilbenes having dimethylene, dioxyl, and dinitroxide centers in *o,o'*-, *o,m'*-, *o,p'*-, *m,m'*-, *m,p'*-, and *p,p'*-substitution patterns, and the various singlet-triplet energy gaps were computed to predict qualitative ground state spin multiplicities. Singlet and triplet spin states were essentially degenerate in the *m,m'*-isomers of disjoint connectivity, while nondisjoint *o,m'*- and *m,p'*-isomers had triplet computed ground states. Nitroxide-based diradicals showed considerably smaller computational exchange coupling energies than did other diradical models studied. As a tests of these computations, stilbenes with two *N*-*tert*-butyl nitroxide groups at the *o,m'*-, *m,m'*-, and *m,p'*-positions were prepared, and their magnetic properties were studied by ESR and magnetic susceptibility measurements. The *m,m'*- and *m,p'*-isomers were found experimentally to have singlet and triplet ground states, respectively, in accord with the qualitative computed predictions.

Introduction

Recently, there has been substantial interest in the study of molecular-based magnetism. The syntheses of organic radicals and polyradicals have been in progress based on individual strategies.¹ Utilizing intermolecular magnetic coupling in crystals, purely organic radicals with bulk ferromagnetic behavior at cryogenic temperature have been studied.² Parallel to these efforts has been another approach to design and synthesize polymeric high-spin organic molecules^{3,4} using long-range intramolecular magnetic coupling. The latter approach involves the application of theoretical models of magnetic coupling to conjugated polymers bearing paramagnetic spin centers. Spin states of open-shell conjugated organic molecules have been described by Longuet-Higgins' model,⁵ the Borden-Davidson rule⁶ based on MO theory, and Ovchinnikov's or Klein's formulations⁷ derived from VB theory. A number of organic open-shell molecules composed of plural doublet or triplet centers connected with magnetic exchange coupler moieties, such as phenylene,⁸

diphenylethylene,^{9,10} diphenyldiacetylene,¹¹ and benzophenone^{10b} have been prepared and characterized as experimental tests of the theoretical principles. The various qualitative theories are quite useful for predicting the ground state spin multiplicities of molecules with triplet spin centers such as carbene or nitrene. However, unexpected ground states have been reported for open-shell conjugated molecules composed of nitroxide radicals.^{8a-e} Such behavior even at very low temperature has been ascribed to reduced electronic interaction between unpaired spins of the nitroxides and/or nonplanar geometries of the exchange coupling moiety^{8f,g}.

As part of our investigation of magnetism in organic diradicals and polyradicals, semiempirical computations were carried out at our laboratory to predict the experimental ground state (GS) spin multiplicities for such species. Computational modeling based upon empirical molecular orbital (MO) plus configuration interaction (CI) computations has previously been successful in correctly predicting GS spin multiplicities for a variety of experimentally known diradicals and diradicaloids.¹² In this paper we apply MO-CI semiempirical methods to study stilbene diradicals containing two each of the following doublet spin centers: methylene, oxyl, and nitroxide

[†] University of Massachusetts.

[‡] Waseda University.

[§] Present address: Department of Applied Chemistry, Keio University, Yokohama 223, Japan.

[®] Abstract published in *Advance ACS Abstracts*, June 15, 1994.

(1) *Magnetic Molecular Materials*; Gatteschi, D., Kahn, O., Miller, J. S., Palacio, F., Eds.; Kluwer Academic Publishers: The Netherlands, 1991.

(2) (a) Chiarelli, R.; Novak, M. A.; Rassat, A.; Tholence, J. L. *Nature* **1993**, *363*, 147. (b) Kinoshita, M.; Turek, P.; Tamura, M.; Nozawa, K.; Shiomi, D.; Nakazawa, Y.; Ishikawa, M.; Takahashi, M.; Awaga, K.; Inabe, T.; Maruyama, Y. *Chem. Lett.* **1991**, 1225.

(3) For reviews, see the following: (a) Dougherty, D. A. *Acc. Chem. Res.* **1991**, *24*, 88. (b) Iwamura, H.; Koga, N. *Acc. Chem. Res.* **1993**, *26*, 346.

(4) (a) Nishide, H.; Yoshioka, N.; Kaneko, T.; Tsuchida, E. *Macromolecules* **1990**, *23*, 4487. (b) Nishide, H.; Yoshioka, N.; Inagaki, K.; Kaku, T.; Tsuchida, E. *Macromolecules* **1992**, *25*, 569. (c) Yoshioka, N.; Nishide, H.; Kaneko, T.; Yoshiki, H.; Tsuchida, E. *Macromolecules* **1992**, *25*, 3838. (d) Fujii, A.; Ishida, T.; Koga, N.; Iwamura, H. *Macromolecules* **1991**, *24*, 1077. (e) Miura, Y.; Matsumoto, M.; Ushitani, Y. *Macromolecules* **1993**, *26*, 2628.

(5) Longuet-Higgins, H. C. *J. Chem. Phys.* **1950**, *18*, 265.

(6) Borden, W. T.; Davidson, E. R. *J. Am. Chem. Soc.* **1977**, *99*, 4587.

(7) (a) Ovchinnikov, A. A. *Theoret. Chim. Acta* **1978**, *47*, 297. (b) Misurkin, I. A.; Ovchinnikov, A. A. *Russ. Chem. Rev. (Engl. Transl.)* **1977**, *46*, 967. (c) Klein, D. *J. Pure Appl. Chem.* **1983**, *55*, 299.

(8) (a) Itoh, K. *Chem. Phys. Lett.* **1967**, *1*, 235. (b) Calder, A.; Forrester, A. R.; James, P. G.; Luckhurst, G. R. *J. Am. Chem. Soc.* **1969**, *91*, 3724. (c) Kothe, G.; Denkel, K. H.; Summermann, W. *Angew. Chem. Int. Ed. Engl.* **1970**, *9*, 906. (d) Veciana, J.; Rovira, C.; Crespo, M.; Armet, O.; Domingo, V. M.; Palacio, F. *J. Am. Chem. Soc.* **1991**, *113*, 2552. (e) Ishida, T.; Iwamura, H. *J. Am. Chem. Soc.* **1991**, *113*, 4238. (f) Dvolaitzky, M.; Chiarelli, R.; Rassat, A. *Angew. Chem. Int. Ed. Engl.* **1992**, *31*, 180. (g) Kanno, F.; Inoue, K.; Koga, N.; Iwamura, H. *J. Am. Chem. Soc.* **1993**, *115*, 847. (h) Rajca, A.; Utamapanya, S. *J. Am. Chem. Soc.* **1993**, *115*, 2396.

(9) (a) Murata, S.; Sugawara, T.; Iwamura, H. *J. Am. Chem. Soc.* **1989**, *109*, 1266. (b) Carilla, J.; Julia, L.; Riera, J.; Brillas, E.; Garrido, J. A.; Labarta, A.; Alcalá, R. *J. Am. Chem. Soc.* **1991**, *113*, 8281.

(10) (a) Matsumoto, T.; Ishida, T.; Koga, N.; Iwamura, H. *J. Am. Chem. Soc.* **1992**, *114*, 9952. (b) Ling, C.; Minato, M.; Lahti, P. M.; van Willigen, H. *J. Am. Chem. Soc.* **1992**, *114*, 9959.

(11) (a) Murata, S.; Iwamura, H. *J. Am. Chem. Soc.* **1991**, *113*, 5547. (b) Sasaki, S.; Iwamura, H. *Chem. Lett.* **1992**, 1759.

(12) (a) Lahti, P. M.; Rossi, A. R.; Berson, J. A. *J. Am. Chem. Soc.* **1985**, *107*, 2273. (b) Lahti, P. M.; Ichimura, A. S.; Berson, J. A. *J. Org. Chem.* **1989**, *54*, 958. (c) Lahti, P. M.; Ichimura, A. S. *J. Org. Chem.* **1991**, *56*, 3030.

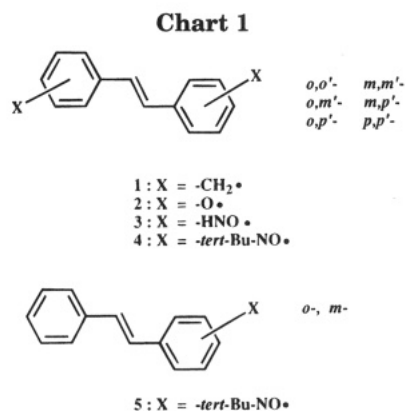


(Chart 1, 1–4). These stilbene derivatives are also dimeric models for related poly(phenylene vinylene) polyradicals. We compared the predictions of the parity rules by comparison to the computed results for 1–4. Then, as experimental tests of the PM3-CI results, o,m' -, m,m' -, and m,p' -stilbenebis(*N*-*tert*-butyl nitroxide) (o,m' -, m,m' -, m,p' -4) were prepared and isolated and their magnetic properties studied by using ESR spectroscopy and magnetic susceptibility measurements.

Computational. The structures of the stilbene diradicals were modeled with the aid of both force field and semiempirical molecular orbital methods. All starting guess geometries were obtained using the MMX force field method^{13a} and were further refined using the PM3^{13b} methodology described in the experimental section. The final PM3 structures were used by us in computations of the relative state energies of the diradicals of interest.

The stilbenes with sterically less bulky radical centers, bis-methylene 1 and dioxy 2, were computed to have planar geometries^{13c} irrespective of their substitution patterns. The system 3 was also planar over the stilbenoid portion of the molecule, but with the NO bond being twisted relative to the plane of the stilbene moiety for all the ortho-substituted nitroxide groups o,o' -, o,m' -, o,p' -3. For the stilbenes 4 with bis(*N*-*tert*-butyl nitroxide) substitution, the N–O bonds formed a dihedral angle of *ca.* 30° relative to the attached phenyl ring in the MMX initial guess geometries, due to steric interference of the bulky *N*-*tert*-butyl groups. This angle for *ortho*-substituted derivatives o,o' -, o,m' -, o,p' -4 increased slightly to *ca.* 50°. These MMX optimized dihedral angles¹³ are well within the wide range of crystallographically reported values for related molecules, such as 11.6° in *N*-*tert*-butylferrocenyl nitroxide¹⁴ and 65.1° and 75.3° in 4,6-dimethoxy-1,3-phenylenebis(*N*-*tert*-butyl nitroxide).^{8g} Apparently, a substantial range of torsion in nitroxide groups may occur in phenyl nitroxide-based molecules, depending upon substitution. Due to the normal uncertainties of force field and semiempirical computations, our own computed torsional angles are somewhat problematic as quantitative predictions. However, the magnitude of torsion found in by our methodology is consistent with experiment. In addition, modest changes in the torsional angles used do not alter the qualitatively

(13) (a) Program MMX-87 by J. J. Gajewski and K. E. Gilbert, Department of Chemistry, Indiana University, Bloomington, IN. (b) Stewart, J. J. P. *J. Comput. Chem.* **1989**, *10*, 209, 221. (c) Geometric results for the MMX-87 force field and PM3 TRIPLET UHF computations described in the experimental section were reasonably similar to one another, although we feel that the PM3 computations give the best results for the geometry about the nitroxide moiety (by comparison to experimental analogues).

(14) Forrester, A. R.; Hepburn, S. P. *Chem. Commun.* **1969**, 698.

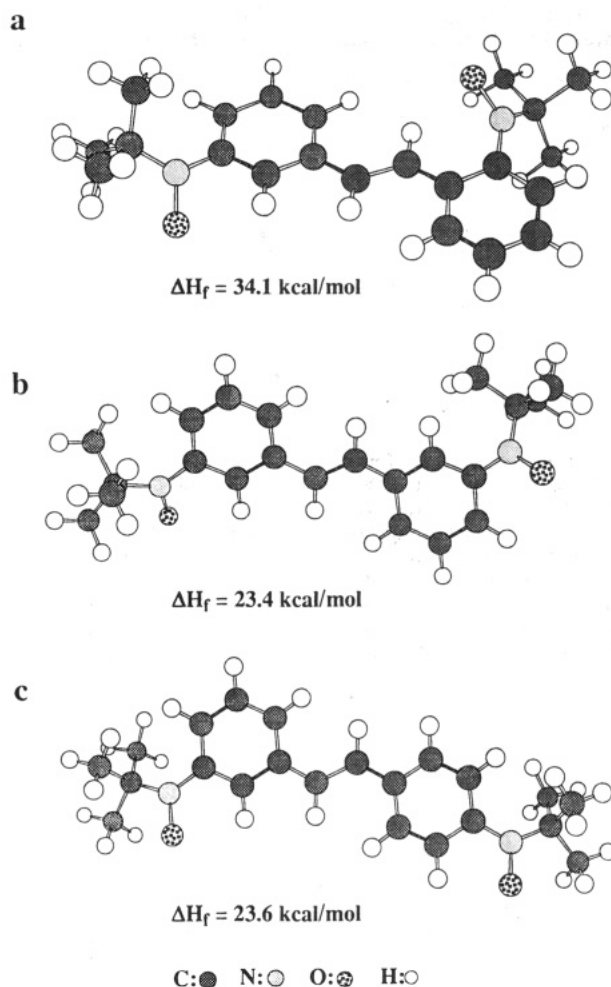


Figure 1. MMX optimized structural diagrams of stilbenebis(*N*-*tert*-butyl nitroxide)s: (a) o,m' -4; (b) m,m' -4; (c) and m,p' -4.

computed ground state spin multiplicity in the cases studied or greatly change the computed T–S gaps.

Structural diagrams for o,m' -, m,m' -, and m,p' -4 are shown in Figure 1.¹³ As in the cases described above, the compound containing an ortho group has a deplanarized nitroxide group. The force field computations for o,m' -4 indicated that this compound has more strain energy than m,m' - and m,p' -4. Although the individual MMX steric energies are not quantitatively significant, the differences in these energies are reflective of different degrees of steric interaction. Using MMX-87, we found m,m' - and m,p' -4 to have nearly the same steric energies (to within 0.3 kcal/mol), while the o,m' -isomer had a steric energy 6–7 kcal/mol higher.

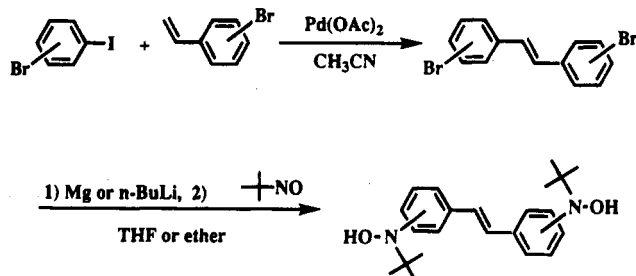
After geometries were obtained for the various diradical derivatives of interest, we assumed them to be fixed for all states, in order to render our computations easier. Next, we used the PM3-CI method^{12b,c} to compute triplet–singlet gaps ΔE_{T-S} for each derivative (Table 1). The results for ground spin states coincided with qualitative, parity-based predictions. While the o,o' -, o,p' -, and p,p' -isomers had computed singlet GSs, the o,m' - and m,p' -isomers had triplet GSs with relatively larger ΔE_{T-S} . Essentially degenerate spin states were found for the m,m' -isomers. 1 and 2 had larger ΔE_{T-S} than that for 3, demonstrating the lesser exchange delocalization in model, planar dinitroxides by comparison to the other types of diradicals investigated. In the case of the

Table 1. Energy Gaps between the Triplet and Singlet States of Stilbene Diradicals Estimated by Semiempirical Calculation

isomer	ΔE_{T-S}^a (kcal/mol)	isomer	ΔE_{T-S}^a (kcal/mol)
<i>o,o'</i> -1	-2.7	<i>m,m'</i> -1	-0.8
2	-7.0	2	-0.9 (0.4) ^b (0.9) ^c
3	-1.2	3	-0.6
4	-0.2 ^d	4	-0.5 ^f
<i>o,m'</i> -1	2.3	<i>m,p'</i> -1	3.3
2	5.0 (2.4) ^b	2	6.9 (-3.1) ^b (6.5) ^c
3	1.2	3	1.6
4	0.6 ^e	4	1.2 ^f
<i>o,p'</i> -1	-3.7	<i>p,p'</i> -1	-4.5
2	-12.5	2	-8.0
3	-1.4	3	-1.8
4	-0.6 ^e	4	-1.2 ^f

^a Estimated by PM3-CI method. $\Delta E_{T-S} > 0$ means triplet GS.

^b Calculated by INDO/CISD method (see ref 12b). ^c Calculated by AM1/CI method (see ref 12c). ^d Optimized planar geometry for *o,o'*-3 was modified using MMX results for *o,o'*-4 ($\langle \text{Ph}-\text{NO} = +50^\circ, \langle \text{Ph}-\text{C}=\text{C} = -10^\circ$). ^e Optimized planar geometries for *o,m'*-, *o,p'*-3 were modified using MMX results *o,m'*-, *o,p'*-, *o,p'*-4 ($\langle \text{Ph}-\text{NO} = +50^\circ, \langle \text{Ph}-\text{C}=\text{C} = -10^\circ, \langle \text{Ph}-m,p-\text{NO} = +30^\circ$). ^f Optimized planar geometries for 3 were modified using MMX results of corresponding 4 (planar stilbene with $\langle \text{Ph}-\text{NO} = +30^\circ$).

Scheme 1

experimentally most realistic systems, bis(*tert*-butyl nitroxide)s 4, ΔE_{T-S} decreased in all isomers compared to analogous ΔE_{T-S} for 3, indicating that electronic interactions through the stilbene conjugated system are weakened by nonplanarity. The larger ΔE_{T-S} values for 2 than those of 1 are conversely attributed to a higher delocalization of spin density onto the phenyl rings in 2 than 1.¹⁵

Syntheses: *E*-Dibromostilbenes were synthesized by using the Heck reaction (Scheme 1). When the appropriate isomers of bromiodobenzene were allowed to react with ring-brominated styrenes in acetonitrile in the presence of a palladium catalyst, the iodinated position was selectively coupled with the vinyl group to yield (*E*)-dibromostilbenes exclusively.¹⁷ These dibromostilbenes showed IR absorptions due to the *trans* HC=CH out-of-plane bending mode at 960–970 cm^{-1} . The stilbenebis(*N*-*tert*-butylhydroxylamine)s (4) were then prepared by coupling¹⁶ of doubly-metalated derivatives of appropriate dibromostilbenes with 2-methyl-2-nitrosopropane. The IR absorption of *o,m'*-4 at 964 cm^{-1} attributed to the *trans*-vinylene moiety was weaker than those of *m,m'*- and *m,p'*-4. We attribute this to a nonplanar geometry between the phenyl ring and the CH=CH group in *o,m'*-4 due to steric interactions of the bulky *N*-*tert*-butyl group, since stilbene itself and *o,m'*-dibromostilbene show strong absorption at 960 cm^{-1} .

Oxidation of the hydroxylamine precursors to compounds of type 4 in benzene or toluene with Ag_2O or PbO_2 gave solutions of the corresponding diradicals, with reddish brown coloring for *o,m'*-4, pale red for *m,m'*-4, and yellowish brown for *m,p'*-4. Mononitroxides *o*- and *m*-5 were prepared *via* reaction sequences analogous to those described above. The formation of diradicals was supported both by new UV-vis absorptions ascribable to alkylaryl nitroxides¹⁶ and by ESR quintet-pattern spectra that are typical for dinitroxides. Spin concentrations of the diradical solutions were determined by careful integration of their ESR signals by comparison to standardized TEMPO solutions. These experiments showed essentially complete oxidation to give diradicals for *m,m'*- and *m,p'*-4, respectively, with 1.99 and 1.98 spin/molecule. We believe that oxidation could also be carried out essentially to completion for *o,m'*-4, though its final spin concentration varied with the reaction conditions used, due to its higher reactivity. Diradicals *m,m'*- and *m,p'*-4 were fairly stable in dilute solution (below 0.2 mM) and their spin concentrations remained constant for a day. In concentrated solution or the neat state, their spin concentrations decreased at a significant rate. An intermolecular disproportionation of the radical was suggested by the appearance of new absorption bands attributed to $=\text{N}^+-\text{O}^-$ at 1625 cm^{-1} , C=O at 1650–1700 cm^{-1} , and NH at 3400 cm^{-1} .^{16a} A fairly rapid decrease in the spin concentration was observed for solutions of the reactive *o,m'*-4, under all conditions attempted, hence this molecule needed to be analyzed by ESR as soon as possible after generation in solution.

ESR Spectra. The ESR spectrum of *o*-5 shows splitting due to typical nitrogen hyperfine coupling ($a_N = 14.2$ G, $I = 1$ yields 1:1:1 intensities), as well as additional proton hyperfine coupling (hfc) (Figure 2). Well-resolved proton hfc was found for *m*-5, indicating appreciable delocalization of spin density onto the phenyl ring. The hfc's were well fit by spectral simulation as $a_N = 12.6$ G, $a_o\text{-H} = 1.9$ G, $a_{m\text{-H}} = 0.8$ G, $a_{p\text{-H}} = 2.1$ G. The spectrum of *m*-5 corresponded very well with the previously reported spectrum of *N*-(3-vinylphenyl)-*N*-*tert*-butyl nitroxide,^{16a} indicating that the proton hfc from the vinylene group and/or the second phenyl ring is negligibly small. The ESR spectra of *o,m'*-, *m,m'*-, and *m,p'*-4 at room temperature all consisted of five lines centered at $g = 2.006$, with a peak-to-peak spacing $\Delta H_{pp} = 6\text{--}7$ G (see Figure 2c for *m,p'*-4). This pattern is consistent with spin exchange between the two unpaired electrons when the interelectronic exchange $J > a_N$.¹⁸ In such cases, a_N is twice ΔH_{pp} , or 12–14 G for our dinitroxides.

All isomers of 4 gave broad and slightly-structured spectra in frozen toluene glass at 77 K (Figure 3), consistent with a weak dipolar interaction between the nitroxide units. It was difficult to simulate the observed frozen spectra, probably in part due to the presence of more than one conformer of each diradical. Half-field $\Delta M_s = 2$ transitions consistent with triplet species were observed at $g = 4$ in each case. These signals were, however, not intense enough to allow the study of their temperature-intensity dependency. Therefore, the ESR signals in the $\Delta M_s = 1$ region were doubly integrated to give Curie Plots. Curie runs were obtained only for samples that were confirmed immediately before freezing

(15) Lloyd, R. V.; Wood, D. E. *J. Am. Chem. Soc.* **1974**, *96*, 659.

(16) (a) Forrester, A. R.; Hepburn, S. P. *J. Chem. Soc. (C)* **1971**, 3322.

(b) Forrester, A. R.; Hepburn, S. P. *J. Chem. Soc. (C)* **1970**, 1277.

(17) (a) Plevyak, J. E.; Dickerson, J. E.; Heck, R. F. *J. Org. Chem.* **1979**, *44*, 4078. (b) Heck, R. F. *Org. React.* **1981**, *27*, 345.

(18) See Wertz, J. E.; Bolton, J. R. *Electron Spin Resonance: Elementary Theory and Practical Applications*; Chapman and Hall: New York, NY, 1986; p 250 ff.

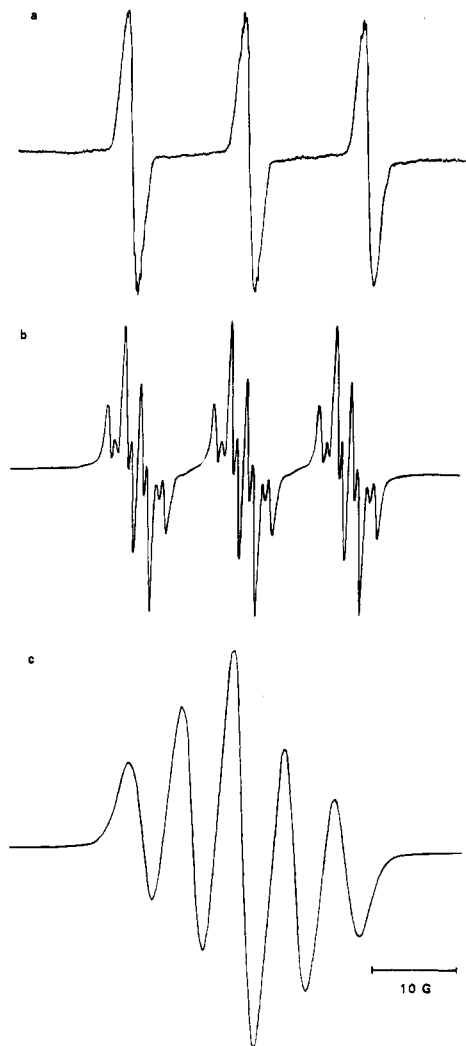


Figure 2. X-Band ESR spectra of stilbene-(*N*-*tert*-butyl nitroxide)s in benzene at room temperature: (a) *o*-5; (b) *m*-5; (c) *m,p'*-4.

to have clean dinitroxide spectra without mononitroxide impurities. While the signal intensity (I) of *m,p'*-4 was essentially proportional to the reciprocal of absolute temperature ($1/T$), the plots for *m,m'*-4 deviated substantially from linearity in the lower temperature region (Figure 4). The intensity data was fitted by nonlinear regression to the usual Bleaney–Bowers type expression¹⁹ given in eq 1:

$$I = (C/T)\{3 \exp(\Delta E_{T-S}/RT)\}/\{1 + 3 \exp(\Delta E_{T-S}/RT)\} \quad (1)$$

where C is a constant to fit the sample intensity and R is 1.987 cal/mol-deg. ΔE_{T-S} was estimated to be -34 cal/mol for *m,m'*-4, where the negative sign denotes a singlet ground state. The good linearity of the fit to the data for *m,p'*-4 is consistent²⁰ with this molecule being a triplet ground state diradical.

Magnetic Susceptibility Studies. The magnetization and static magnetic susceptibilities of *m,m'*- and *m,p'*-4 were measured with a SQUID magnetometer. These diradicals were implanted in diamagnetic polystyrene (4:PS = 1:100 w/w) to minimize intermolecular

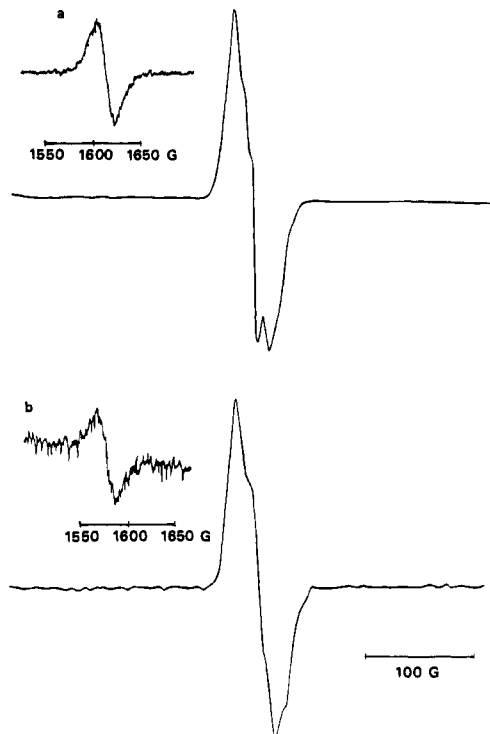


Figure 3. X-Band ESR spectra of stilbenebis(*N*-*tert*-butyl nitroxide)s in toluene glass: (a) *m,m'*-4; (b) *m,p'*-4.

magnetic interactions and to suppress the degradation of radical or the decrease in spin concentration. The ratio μ_{eff}/μ_B was calculated from eq 2:

$$\mu_{\text{eff}}/\mu_B = (3kT\chi/N_A)^{1/2}/\mu_B \quad (2)$$

where χ , k , N_A , and μ_B are molar paramagnetic susceptibility, the Boltzmann constant, the Avogadro number, and the Bohr magneton, respectively. Plots of χ and μ_{eff}/μ_B vs T for *m,m'*-4 are shown in Figure 5. The μ_{eff}/μ_B curve for *m,m'*-4 was in good agreement with the value of $S = 1/2(\mu_{\text{eff}}/\mu_B = 2.45)$ in the high-temperature region. The solid line in Figure 5 shows the calculated χ curve for the Bleaney–Bowers¹⁹ expression relating χ and temperature (eq 3) at $\Delta E_{T-S} = -27$ cal/mol:

$$\chi = 2N_{Ag}^2 \mu_B^2 / kT(3 + \exp(-\Delta E_{T-S}/RT)) \quad (3)$$

A minor deviation of the data from the calculated curve at low temperatures indicates minor intermolecular interaction or a paramagnetic sample component.

(20) Strictly speaking, the observation of a linear Curie-type variation of spectral intensity as a function of reciprocal absolute temperature is dependent upon the assumption that rapid equilibrium between ground and thermally excited states of different multiplicity is maintained (cf. Reynolds, J. H.; Berson, J. A.; Kumashiro, K.; Duchamp, J. C.; Zilm, K. W.; Rubello, A.; Vogel, P. *J. Am. Chem. Soc.* **1992**, *114*, 763 and Bush, L. C.; Heath, R. B.; Berson, J. A. *J. Am. Chem. Soc.* **1993**, *115*, 9830.). Presumably this criterion is readily met in dinitroxides, since the spin-orbit coupling moments of the heteroatoms should enhance intersystem crossing rates. More pernicious is the fact that linear Curie law behavior may be observed for systems with extremely small (degenerate) energy gaps between ground and excited states, as well as for systems with quite substantial gaps. Inherent limitations of interpreting Curie-type experiments with ESR spectroscopy are described by Berson, J. A. In *The Chemistry of the Quinonoid Compounds*: Patai, S., Rappaport, Z., Eds.; Wiley: New York, 1988; pp 462 ff. Some cases of ground state multiplicity deduction by Curie analysis, in which Hund's rule as interpreted for molecules is apparently violated, are discussed in Borden, W. T.; Iwamura, H.; Berson, J. A. *Acc. Chem. Res.* **1994**, *27*, 109.

(19) Bleaney, B.; Bowers, K. D. *Proc. R. Soc. London* **1952**, *A214*, 451.

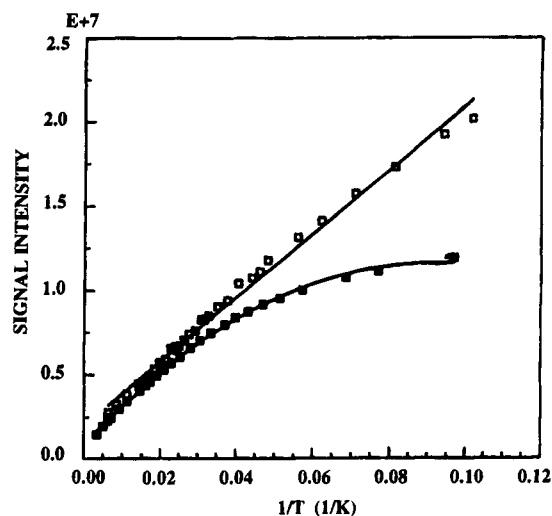


Figure 4. Curie plots for the peak in $\Delta M_s = 1$ region for m,m' -4 (■) and m,p' -4 (□).

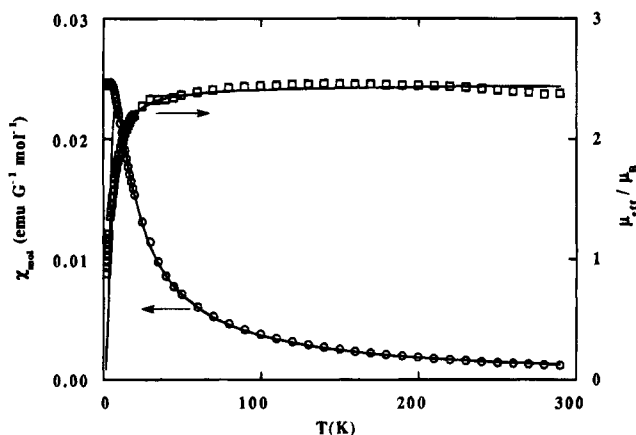


Figure 5. χ and μ_{eff}/μ_B vs T plots for m,m' -4. Solid lines are theoretical curves calculated using eq 3 with $\Delta E_{T-S} = -27$ cal/mol.

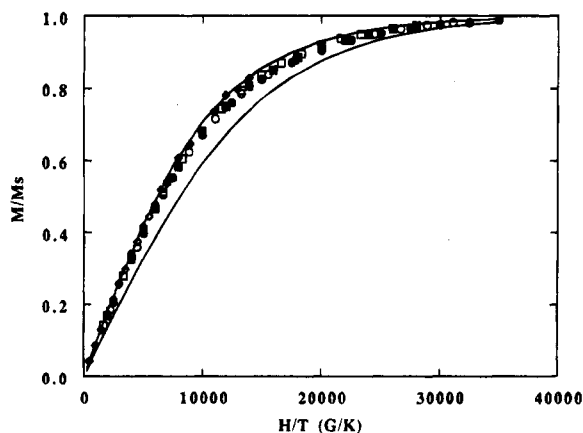


Figure 6. Normalized plots of magnetization (M/M_s) vs the ratio of magnetic field and temperature for m,p' -4: 2 K (●), 2.25 K (○), 2.5 K (■), 3 K (□), 5 K (◆) and 10 K (◇). The solid lines are the Brillouin curves for $S = 1/2$ and $S = 1$.

Magnetization plots of m,p' -4 normalized for saturated magnetization are shown in Figure 6. These plots fall between the theoretical Brillouin curves for $S = 1/2$ and $S = 1$ at 2–10 K. The plots at 5 and 10 K follow very closely the theoretical curve for $S = 1$, indicating a triplet GS for m,p' -4. The slight deviation at lower temperature

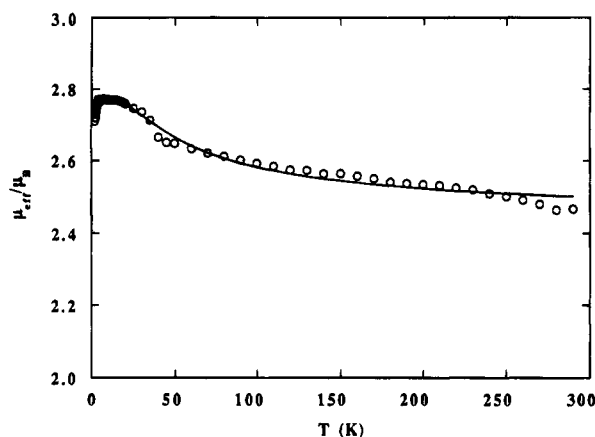


Figure 7. μ_{eff}/μ_B vs T data of m,p' -4. The solid line is the theoretical curve calculated using eq 4 with $\Delta E_{T-S} = 117$ cal/mol, $\theta = -0.10$ K, and $x = 0.11$.

is ascribed to intermolecular antiferromagnetic interactions. We find μ_{eff}/μ_B of m,p' -4 to be ca. 2.5 at high-temperature region, an intermediate value between the values of $\mu_{\text{eff}}/\mu_B = 2.45$ and 2.83 that are expected for $S = 1/2$ and 1, respectively (Figure 7).

The μ_{eff}/μ_B value for m,p' -4 could be corrected by the spin concentration 1.67 spin/molecule, determined from the saturated magnetization at 2 K. Therefore eq 2 was corrected to $\mu_{\text{eff}}/\mu_B = (3kT_x/0.835N_A)^{1/2}/\mu_B$. By adding this correction to account for doublet monoradical species in the triplet sample, eq 3 was modified to give eq 4, where

$$\mu_{\text{eff}}/\mu_B = \left(\frac{6g^2T}{(T - \Theta)(3 + \exp(-\Delta E_{T-S}R/T))} (1 - x) + \frac{3g^2T}{2(T - \Theta)} x \right)^{1/2} \quad (4)$$

θ and x are the Weiss constants for intermolecular magnetic interaction and the fraction of the doublet species in m,p' -4, respectively. Curve fitting of the data to eq 4 yields $\Delta E_{T-S} = 117 \pm 4$ cal/mol, $\Theta = 0.10 \pm 0.02$, $x = 0.11 \pm 0.01$. Thus, about 10% of monoradical impurities was present in the sample of m,p' -4.

Discussion

Several useful qualitative models for describing and predicting ground spin states of open-shell organic molecules have been proposed.²¹ Longuet-Higgins⁵ showed by applying Hückel theory to planar alternant systems with N p -centers and T double bonds in the structure of highest Kekulé bondedness that the number of nonbonding molecular orbitals (NBMOs) is given by eq 5.

$$\text{no. of NBMO} = N - 2T \quad (5)$$

On the basis of Hund's rule, a molecule with two NBMOs should possess a triplet GS. For most alternant molecules, the number of NBMOs is to a first approximation properly predicted by eq 5, except for $4n$ annulenes.

Borden and Davidson⁶ noted that Coulombic repulsion between unpaired electrons would be quite small if the two NBMOs of a diradical could be confined to separate regions of the molecule, hence minimizing ΔE_{T-S} . This

(21) For reviews, see (a) Borden, W. T. *Diradicals*; Wiley: New York, 1982. (b) Berson, J. A. In *The Chemistry of the Quinonoid Compounds*; Patai, S., Rappaport, Z., Eds.; Wiley: New York, 1988; Vol. 2, Part 1, Chapt. 10.

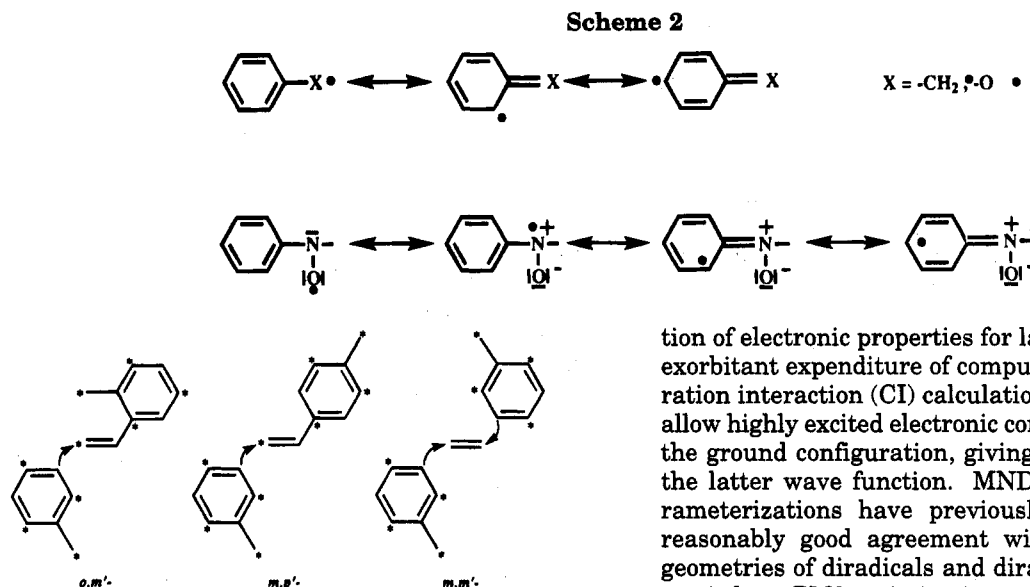


Figure 8. Connectivity patterns for the stilbene isomers with expected open shell electronic states.

Table 2. Expected Spin State for Stilbene-bis-methylenes

isomer	no. of NBMO	$S = n^* - n^0 /2$	connectivity for NBMO
<i>o,o'</i> -1	0	0	
<i>o,m'</i> -1	2	1	nondisjoint
<i>o,p'</i> -1	0	0	
<i>m,m'</i> -1	2	0	doubly disjoint
<i>m,p'</i> -1	2	1	nondisjoint
<i>p,p'</i> -1	0	0	

kind of π -system is said to be disjoint. When the NBMOs cannot be localized in different regions of the diradical, a π -system is called nondisjoint and is expected to have a high-spin GS with a substantial energy gap ΔE_{T-S} .

For an alternant π -system with $n^* > n^0$, Ovchinnikov's model has been used to predict the GS spin quantum number S , as given in eq 6.^{7a,b}

$$S = (n^* - n^0)/2 \quad (6)$$

A similar relationship with a more rigorous derivation has also been given by the work of Klein.^{7c} The most attractive feature of this formulation is the finding of GS spin multiplicity by simple enumeration of the molecular connectivity. The formulation has also been applied to heteroatom-containing molecules.

Using these principles, the electronic ground states of stilbenebis(methylene)s may be predicted as shown in Table 2. For the *o,o'*-, *o,p'*-, and *p,p'*-isomers eqs 5 and 6 predict singlet GSs (valence bonding considerations additionally predict quinonoidal bonding patterns), while triplet GSs are predicted for the *o,m'*- and *m,p'*-isomers. On the other hand, the *m,m'*-isomer possesses π -centers which are connected by the $-\text{CH}=\text{CH}-$ linker unit across nodal sites of the radical-bearing ring moieties: a singlet GS with small ΔE_{T-S} is expected for such a disjoint system (Figure 8). Simple qualitative principles such as those just outlined are effective to distinguish favorable spin state in a π -system, but do not allow any clear insight into a magnitude of the energy gap nor comparison of the magnetic coupling strength among various systems.

Semiempirical molecular orbital methods rely on parameterization from experimental data to allow predic-

tion of electronic properties for large molecules, without exorbitant expenditure of computational time. Configuration interaction (CI) calculations then may be used to allow highly excited electronic configurations to mix with the ground configuration, giving a better description of the latter wave function. MNDO, AM1, and PM3 parameterizations have previously been found to give reasonably good agreement with *ab initio* computed geometries of diradicals and diradicaloids.¹² Hence, we carried out PM3 optimizations on the various diradicals 1–4 using the TRIPLET UHF option in MOPAC.²² We then performed CI using the 1SCF MECI OPEN(2,2) C.I.= (5,2) MS=O keyword set to obtain both triplet and singlet state energies of the diradicals, assuming the same fixed geometry for both. The ΔE_{T-S} values calculated by this procedure are given in Table 1. The calculated values for stilbene diradicals from PM3-CI were quite similar to those from AM1-CI.^{12a} The PM3-CI method did not yield the puzzling open-shell singlet GS which was estimated by INDO/CISD^{12b} for *m,p'*-2. As mentioned above, all systems for which $n^* > n^0$ in eq 6 were computed to have high spin ground states. In addition, PM3-CI predicts singlet GSs by small energetic margins for the doubly disjoint *m,m'*-systems.

The smaller ΔE_{T-S} values that were computed for 3 and 4 by comparison to those for 1 and 2 are explicable in terms of the substantial localization of spin density distribution in the nitroxide N–O bond (Scheme 2). The spin densities on nitrogen and oxygen in dialkyl nitroxides have been determined by their anisotropic coupling constants to be $\rho_N \approx \rho_O \approx 0.5$. The sum of the spin densities in the phenyl ring of *N-tert-butyl N-phenyl nitroxide* has been estimated to be 0.1,²³ which was much smaller than that found in the connectivity-related benzyl (0.3)^{24a} and phenoxy radicals (0.6).^{24b} Furthermore, delocalization of the spin density into the phenyl ring decreases ρ_N but does not affect ρ_O . Finally, the non-coplanar arrangement in 4 between the N–O bond and the attached phenyl ring further increases the localization of unpaired electron in the nitroxide unit.

The comparative extent of delocalization of unpaired spin density in the stilbene dinitroxides is also shown by the ESR spectra of monosubstituted radicals *o*- and *m*-5. The ESR of *o*-5 has a higher a_N value and smaller ring-proton hfc constants than those of *m*-5 and the corresponding *para* isomer reported by Forrester.^{16a} Similar values of a_N and a_H that have been reported for *o*-alkylaryl nitroxides are consistent with localization of spin density on the N–O bond in response to the increase in the twisting angle between N–O bond and phenyl

(22) Dewar, M. J. S.; Stewart, J. J. P. QCPE 504.

(23) Aurich, H. G.; Hahn, K.; Stork, K.; Weiss, W. *Tetrahedron* **1977**, *33*, 969.

(24) (a) Carrington, A.; Smith, I. C. P. *Mo. Phys.* **1965**, *9*, 137. (b) Müller, E.; Eggenberger, H.; Rieker, A.; Scheffler, K.; Spanagel, H. B.; Stegmann, H. B.; Teissier, B. *Tetrahedron* **1965**, *21*, 227.

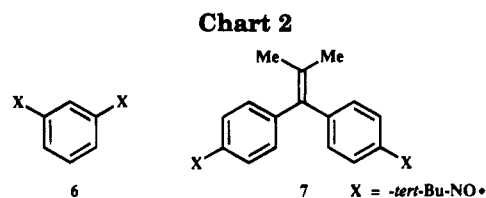
plane. The similarity of the ESR proton hfc constants in *m*-5 and *m*-styryl *N*-*tert*-butyl nitroxide^{16a} supports the localization of spin distribution in one phenyl ring suggests similar localization in the disjoint molecule *m,m'*-4.

Although the solution phase, spin-exchanged ESR spectra of *o,m'*-, *m,m'*-, and *m,p'*-4 were virtually the same, the five-line spectrum for *o,m'*-4 gradually changed to a three-line spectrum ascribable to a mononitroxide, indicating chemical degradation of *o,m'*-4. Since there was no resolvable proton-hfc, the extent of delocalization of the unpaired electrons could not be determined from the spectra of *o,m'*-4.

The observed instability of the nitroxides in concentrated solution or in the neat state appears to be caused by an intermolecular disproportionation reaction between two nitroxides to give an amine and quinone imine *N*-oxide. For instance, the rapid deterioration of *o,m'*-4 is analogous to the intramolecular disproportionation reported for *N*-*tert*-butyl-(*o*-vinylphenyl)nitroxide.^{16b} As a result, all studies were carried out at once upon samples freshly made by oxidation, to avoid byproduct contamination that occurs upon standing.

The magnetization and μ_{eff}/μ_B plots of *m,m'*- and *m,p'*-4 indicate singlet and triplet GS for these connectivities, respectively. The triplet-singlet energy gaps are determined to be $-27 < \Delta E_{T-S} < 0$ cal/mol for *m,m'*-4 and $\Delta E_{T-S} = 117 \pm 4$ cal/mol for *m,p'*-4, respectively. ΔE_{T-S} was independently estimated by the thermal dependence of the ESR signal intensity of the $\Delta M_s = 1$ peak for disjoint *m,m'*-4 to be -34 cal/mol, in reasonable agreement with the value of -27 cal/mol found by magnetic susceptibility measurement. Due to the experimental limitations of temperature control in the ESR experiment, the value from the magnetic susceptibility is presumed to be more accurate, but the agreement of ΔE_{T-S} from the two methods helps further to fix the small magnitude of ΔE_{T-S} in this case.

The experimental ΔE_{T-S} of *m,m'*- and *m,p'*-4 qualitatively agree with the semiempirical ground state predictions shown in Table 1, but are smaller than the computational predictions. The computed value of ca. 0.5 kcal/mol for disjoint *m,m'*-4 is about 1 order of magnitude larger than observed. For the nondisjoint system *m,p'*-4, $\Delta E_{T-S} = 117$ cal/mol is likewise smaller than either the computed value of > 1 kcal/mol or the experimental value for related nondisjoint *m*-phenylenebis(*N*-*tert*-butyl nitroxide) (**6**) ($J/k > 300$ K ≈ 0.6 cal/mol).^{9a} However, this value is smaller than that for 2,2-dimethyl-1,1-ethenediylbis[*p,p'*-(*N*-*tert*-butyl phenyl nitroxide)] (**7**) ($\Delta E_{T-S} = 30.3$ cal/mol).^{10a} Since almost the same dihedral angle between the N—O bond and the phenyl ring is found for the latter two molecules, the difference in ΔE_{T-S} apparently depends on other geometric and/or electronic factors. In **6**, the two *N*-*tert*-butyl nitroxide groups are coupled through a single phenyl ring, giving the largest ΔE_{T-S} gap among the set of dinitroxides *m,p'*-4, **6**, and **7**. Since nine sp^2 carbons separate the two nitroxide groups both in *m,p'*-4 and **7**, the main difference between these two is the nonplanar geometry in **7** about the sterically crowded 2-methylpropene moiety. *m,p'*-4 apparently allows better through-bond coupling between the two radical centers because its stilbene structure preserves planarity, as predicted by our calculations. A geometrically very distorted stilbenoid diradical variant, *trans*-perchlorovinylenebis($\alpha,\alpha,\alpha',\alpha'$ -tetraphenyl-1,3-xylylene), has been reported to yield exchange coupling



behavior indicative of two isolated radical centers^{9b} rather than a diradical. These findings demonstrate that magnetic interaction of weakly coupled diradicals may be strongly affected by the geometry of the unit that links the radical centers, as well as the by the degree of conjugation of the radical centers to the linking structural unit.

The comparison between experiment and theory highlights both the weaknesses and strengths of computational modeling of open-shell molecules. In a semiquantitative manner, the computations are quite successful. Molecular geometries are obtained that are in good accord with experimental model results. Qualitative ground state multiplicities are predicted that agree with those observed. A good notion may be obtained, concerning the relative strength of exchange coupling for different types of related diradical models: for instance, dinitroxides are computationally found to give weaker coupling than a number of other diradicals of the same connectivity, consistent with the known propensity of dinitroxides to be localized. It even appears possible to get useful predictions of whether ΔE_{T-S} is "large" (> 5 kcal/mol) or "small" (≤ 1 kcal/mol). However, precise predictions of ΔE_{T-S} to ± 1 kcal/mol or better is not possible, as shown by comparison of the actual experimental values to computational predictions. Given that such predictive precision is possible even at the ab initio level of computational methods only for very small molecules, we feel that the comparison between semiempirical and experimental numbers obtained by us to be surprisingly good. When one considers the additional simplifying assumptions made by us in the computations, the agreement is even more impressive. For example, we have not accounted explicitly for difference in the geometry of ground vs excited states in our ΔE_{T-S} calculations. Also, we are using a limited CI treatment with a semiempirical methodology that is not explicitly fit to agree with diradical data. Limited CI computations are not size-consistent, hence a single scheme may not apply with equal accuracy to prediction of the electronic nature and energies of all states for molecules of differing size. All of these factors have been noted in previous work that employs these methods for open-shell molecules.¹²

Despite all the caveats, we obtain results in good agreement with experiment, as we have previously. We consider this to be yet another example of the utility of a semiempirical methodology (which has been carefully calibrated against known experimental data) being extrapolated to investigation of a limited experimental variable—in this case, the strength of exchange interaction in conjugated diradicals as a function of spin-bearing site for stilbenoid-linked systems. While semiempirical MO-CI methods should not be interpreted as giving infallibly precise predictions of properties for any single given molecule, they are useful and convenient guides to explore trends among whole classes of structurally related molecules, and with modern improvements in parameterization and procedures have proven their

usefulness as aids to the understanding and classifying of diradicals and related open-shell molecules.

Conclusion

We find that use of PM3-CI calculations at PM3-UHF optimized geometries was effective to predict the ground state spin multiplicities of stilbenoid diradicals in accord with qualitative theoretical principles and with experimental results. The π -isoelectronic replacement of methylene radical sites with heteroatom spin-bearing sites (oxyl and nitroxide) does not change the qualitative ground state predictions, but the use of nitroxide centers leads to a prediction of a decrease in magnetic interaction through stilbene π -system due to the localization of unpaired spin density on the N—O bond.

The magnetic properties of stilbenebis(*N*-*tert*-butyl nitroxide) diradical models for our computations were studied. The m,m' - and m,p' -isomers were relatively stable, while the o,m' -isomer degraded within a couple of hours. Temperature dependencies of their magnetic susceptibilities indicated singlet and triplet ground states for the m,m' - and the m,p' -isomer, respectively, in accord with computation and with qualitative expectations. Polyradicals composed of stilbenoid units with nondisjoint connectivity of spin centers are expected to show intramolecular ferromagnetic coupling along the chain.

Experimental Section

Computational Methods. Initial guess geometries using the MMX force field calculations (full SCF, triplet state calculation, para electrons included) were carried out on an IBM clone 486-class personal computer using PCMODEL.²⁵ More complete MMX-87²⁵ molecular mechanics optimizations were then performed on a Digital Equipment Corporation VAX at the University of Massachusetts (Amherst) Computer Center. As a final step, the MMX structures were optimized with MOPAC (version 6.0) using the PM3 UHF TRIPLET keyword set. After the PM3 optimizations, the geometry of each diradical was frozen and configuration interaction (CI) computations of the triplet and singlet energies carried out by a variation of a standard CI procedure used by us.^{12b,c}

ESR Spectroscopic Measurements. ESR spectra were taken on a Bruker ESP-300 ESR and a JEOL JES-2XG ESR spectrometer with 100-kHz field modulation in the X-band frequency region. Spin concentrations in each solution sample were determined by careful double integration of the ESR signal versus a standard concentration of 2,2,6,6-tetramethyl-1-piperidineoxyl (TEMPO) solution.²⁶ Signal positions were calibrated against an external standard of diphenylpicrylhydrazyl radical ($g = 2.0037$).

Temperature dependency of the ESR spectral intensities was measured using an APD Cryogenics CS-202 Displex closed-cycle circulating helium cryostat. Freshly prepared samples of the appropriate stilbene dinitroxide in benzene were mixed with Fluorolube (4/Fluorolube = 1/100 w/w) and evaporated. The resultant oily mull was coated on the OHFC copper rod sample spindle of the Displex apparatus inside an APD Cryogenics DMX-15 ESR Suprasil shroud, the apparatus evacuated to less than 10 mm Hg, and cooling commenced. The temperature of the samples in method 2 could be monitored at the base of the Displex cooling stage, using an iron-doped gold—chromel thermocouple (Scientific Instruments, Inc. Model CG07FC-4). A correction to this temperature could then be applied based upon calibration experiments in which an

additional thermocouple was attached to the portion of the sample spindle that was to be situated within the ESR sample cavity. The spectra were recorded at various temperatures and double-integrated by standard procedures using a standard Bruker software. Plots of the integrated intensity vs inverse temperature were analyzed by nonlinear least-squares methods using the PS-Plot program (Polysoft, Salt Lake City, UT) on an IBM clone 80486 personal computer.

IR, NMR, and mass spectra were measured with a JASCO FT/IR-5300, a GE NMR Instruments Omega 500, and a Shimadzu GC-MS QP-1000 spectrometer, respectively.

Thermal gravimetric analysis (TGA) and differential thermal analysis (DTA) with Seiko Instruments Inc. TG/DTA 220 were used to measure melting points at a rate of 10 °C/min under nitrogen.

Magnetic Measurement. Magnetization and static magnetic susceptibility were measured with a Quantum Design MPMS SQUID magnetometer. The magnetization was measured from 5000 G to 70000 G at 2, 2.25, 2.5, 3, 5, and 10 K. The static magnetic susceptibility was measured over 2–300 K in a field of 5000 G.

Synthetic. General Procedure for (*E*)-Dibromostilbenes. Each dibromostilbene was synthesized from the corresponding bromostyrene and bromiodobenzene by Heck reaction.¹⁷ A volume of 0.044 g (0.2 mmol) of palladium acetate and 5 g (50 mmol) of triethylamine were added to an acetonitrile solution (10 mL) of 1.8 g (10 mmol) of bromostyrene and 2.8 g (10 mmol) of bromiodobenzene under nitrogen atmosphere and the solution was stirred for 12 h at 80 °C. The solution was evaporated, washed with 10% aqueous hydrochloric acid, and extracted with ether. After drying over anhydrous sodium sulfate, the ether solution was evaporated and developed on a silica gel column with hexane or chloroform/hexane.

***o,m'*-Dibromostilbene** was prepared from *o*-bromostyrene and *m*-bromiodobenzene: yield 61%; mp 33–35 °C; IR (KBr pellet, cm^{-1}) 960 (δ *trans*-HC=CH); MS (m/z) 336, 338, 340 (M^+ , $M^+ + 2$, $M^+ + 4$), calcd $M = 338.04$. Anal. Calcd for $\text{C}_{14}\text{H}_{10}\text{Br}_2$: C, 49.7; H, 3.0; Br, 47.3. Found: C, 49.6; H, 3.1; Br, 47.4.

***m,m'*-Dibromostilbene** was prepared from *m*-bromostyrene and *m*-bromiodobenzene: yield 60%; mp 107 °C (lit.²⁷ 108–110 °C); IR (KBr pellet, cm^{-1}) 970 (δ *trans*-HC=CH); MS (m/z) 336, 338, 340 (M^+ , $M^+ + 2$, $M^+ + 4$), calcd $M = 338.04$. Anal. Calcd for $\text{C}_{14}\text{H}_{10}\text{Br}_2$: C, 49.7; H, 3.0; Br, 47.3. Found: C, 50.1; H, 3.0; Br, 47.5.

***m,p'*-Dibromostilbene** was prepared from *m*-bromostyrene and *p*-bromiodobenzene: yield 54%; mp 88 °C; IR (KBr pellet, cm^{-1}) 970 (δ *trans*-HC=CH); MS (m/z) 336, 338, 340 (M^+ , $M^+ + 2$, $M^+ + 4$), calcd for $M = 338.04$. Anal. Calcd for $\text{C}_{14}\text{H}_{10}\text{Br}_2$: C, 49.7; H, 3.0; Br, 47.3. Found: C, 49.8; H, 3.0; Br, 47.3.

(*E*)-Stilbenebis(*N*-*tert*-butylhydroxylamine)s. These hydroxylamines described below were prepared by the coupling reaction of dilithiated stilbenes or stilbene bis(magnesium bromide) with 2-methyl-2-nitrosopropane.

***o,o'*-Stilbenebis(*N*-*tert*-butylhydroxylamine):** 1.7 g (5 mmol) of dibromostilbene in 10 mL of THF was added to 0.24 g (10 mmol) of dried magnesium in the presence of a few drops of 1,2-dibromoethane as a reaction initiator under nitrogen atmosphere, and the solution was heated at reflux until the magnesium was completely reacted. After cooling, 3.4 g (20 mmol) of 2-methyl-2-nitrosopropane in THF was added to the Grignard reagent, and the mixture was stirred for 1 h at room temperature. The reaction mixture was treated with aqueous ammonium chloride, extracted with chloroform, and washed with water. The chloroform layer was dried over anhydrous sodium sulfate. After evaporation, the crude product was recrystallized from chloroform/hexane: yield 21%; mp 201 °C dec;²⁸ IR (KBr pellet, cm^{-1}) 3256 (ν *o*-H), 964 (δ *trans*-HC=CH); ¹H-NMR (DMSO-*d*₆, 500 MHz; ppm) δ 0.206 (s, 9H), 0.265 (s,

(27) Kruger, K.; Lippert, E. *Chem. Ber.* **1969**, *102*, 3233.

(28) Thermal gravimetric analysis (TGA) and differential thermal analysis (DTA) for *o,m'*-4 at a rate of 10 °C/min showed an exothermic peak and weight loss, suggesting decomposition at 201 °C without endotherm ascribed to melting.

(25) Program PCMODEL was purchased from Serena Software, P.O. Box 3076, Bloomington, IN 47402-3076. The VAX version of MMX obtained through Serena Software from Prof. K. Steliou, Université de Montréal, Montréal, Québec.

(26) Cf. Ranby, B.; Rabek, J. F. *Electron Spin Resonance Spectroscopy in Polymer Research*; Springer-Verlag: Berlin, Germany, 1977; pp 41–43.

9H), 6.21 (d, 1H, $J = 7.7$ Hz), 6.23 (d, 1H, $J = 16.6$ Hz), 6.30 (t, 1H, $J = 7.7$ Hz), 6.33 (d, 1H, $J = 7.7$ Hz), 6.39 (t, 1H, $J = 7.7$ Hz), 6.39 (t, 1H, $J = 7.7$ Hz), 6.62 (s, 1H), 6.65 (d, 1H, $J = 7.7$ Hz), 6.84 (d, 1H, $J = 7.7$ Hz), 6.92 (d, 1H, $J = 16.6$ Hz), 7.45 (s, 1H), 7.56 (s, 1H); $^{13}\text{C-NMR}$ (DMSO- d_6 , ppm) δ 25.28, 25.53, 58.87, 59.81, 120.57, 122.20, 123.08, 123.46, 124.65, 125.54, 125.60, 125.91, 126.54, 127.17, 132.59, 136.35, 147.84, 150.75; MS (m/z) 354 (M^+), calcd for $M = 354.48$. Anal. Calcd for $\text{C}_{22}\text{H}_{30}\text{N}_2\text{O}_2$: C, 74.5; H, 8.5; N, 7.9. Found: C, 73.6; H, 8.6; N, 7.9; Br, <0.2.

***m,m'*-Stilbenebis(*N*-*tert*-butylhydroxylamine)**: 1.7 g (5 mmol) of dibromostilbene in 10 mL of THF was added to 0.24 g (10 mmol) of dried magnesium in the presence of a few drops of 1,2-dibromoethane under nitrogen, and the solution was heated at reflux. After cooling, 3.4 g (20 mmol) of 2-methyl-2-nitrosopropane in THF was added to the Grignard reagent, and the mixture was stirred for 1 h at room temperature. The mixture was treated with aqueous ammonium chloride, extracted with chloroform, and washed with water. The chloroform layer was dried and evaporated. The crude product was recrystallized from chloroform: yield 40%; mp 240 °C; IR (KBr pellet, cm^{-1}) 3221 (ν *o*-H), 963 (δ *trans*-HC=CH); $^1\text{H-NMR}$ (DMSO- d_6 , 500 MHz; ppm) δ 0.29 (s, 18H), 6.28 (d, 2H, $J = 7.8$ Hz), 6.36 (s, 2H), 6.42 (t, 2H, $J = 7.8$ Hz), 6.50 (d, 2H, $J = 7.8$ Hz), 6.60 (s, 2H), 7.49 (s, 2H); $^{13}\text{C-NMR}$ (DMSO- d_6 , ppm) δ 25.74, 58.97, 121.85, 122.03, 123.29, 127.23, 128.05, 136.00, 150.75; MS (m/z) 354 (M^+), calcd for $M = 354.48$. Anal. Calcd for $\text{C}_{22}\text{H}_{30}\text{N}_2\text{O}_2$: C, 74.5; H, 8.5; N, 7.9. Found: C, 74.3; H, 8.8; N, 7.8; Br, <0.2.

***m,p'*-Stilbenebis(*N*-*tert*-butylhydroxylamine)**: 30 mL of 1.5 *M* *n*-butyllithium solution in hexane (45 mmol) was added to 1.7 g (5 mmol) of dibromostilbene in 80 mL of ether at -70 °C. After the solution was stirred for 3 h at room temperature, 4.4 g (50 mmol) of 2-methyl-2-nitrosopropane was added at 0 °C, stirred for 1 h at room temperature, and heated at reflux for 15 min. After cooling, the solution was washed with aqueous ammonium chloride and then with water. The ether layer was dried over anhydrous sodium sulfate. After evaporation, the crude product was recrystallized from chloroform/hexane (1/2): yield 6%; mp 205 °C; IR (KBr pellet, cm^{-1}) 3242 (ν *o*-H), 959 (δ *trans*-HC=CH); $^1\text{H-NMR}$ (DMSO- d_6 , 500 MHz; ppm) δ 0.23 (s, 9H), 0.24 (s, 9H), 6.22 (d, 1H, $J = 7.7$ Hz), 6.27 (s, 2H), 6.33 (d, 2H, $J = 8.7$ Hz), 6.38 (t, 1H, $J = 7.7$ Hz), 6.43 (d, 1H, $J = 7.7$ Hz), 6.52 (s, 1H), 6.62 (d, 2H, $J = 8.7$ Hz), 7.45 (s, 1H), 7.46 (s, 1H); $^{13}\text{C-NMR}$ (DMSO- d_6 , ppm) δ 25.67, 58.92, 59.19, 121.62, 121.80, 123.06, 123.88, 125.18, 127.08, 127.19, 127.44, 132.44, 136.15, 149.93, 150.69; MS (m/z) 354 (M^+), calcd for $M = 354.48$. Anal. Calcd for $\text{C}_{22}\text{H}_{30}\text{N}_2\text{O}_2$: C, 74.5; H, 8.5; N, 7.9. Found: C, 74.3; H, 8.8; N, 7.7; Br, <0.2.

Stilbenebis(*N*-*tert*-butyl nitroxide)s (4): 17.7 mg (0.05 mmol) of stilbene-bis-(*N*-*tert*-butylhydroxylamine) in 50 mL of

toluene or benzene was treated with 0.23 g (1 mmol) of Ag_2O or PbO_2 . After filtration, the benzene solution was freeze-dried. The benzene solution of stilbenebis(*N*-*tert*-butyl nitroxide) was added to a benzene solution of a certain amount of purified polystyrene (molecular weight 2×10^5) or Fluorolube and stirred under nitrogen atmosphere. Freeze-drying of the solution gave flake and oily samples diluted with the diamagnetic polystyrene or Fluorolube.

***N*-*tert*-Butyl *N*-(β -phenylvinyl)phenyl nitroxides 5**. These hydroxylamines were prepared by the coupling reaction of monolithiated stilbenes or stilbene magnesium bromide with 2-methyl-2-nitrosopropane in the same way described above.

***o*-Stilbene-*N*-*tert*-butylhydroxylamine**: yield 5%; mp 134 °C; IR (KBr pellet, cm^{-1}) 3244 (ν *o*-H), 963 (δ *trans*-HC=CH); $^1\text{H-NMR}$ (CDCl_3 , 500 MHz; ppm) δ 1.17 (s, 9H), 5.28 (s, 1H), 6.99 (d, 1H, $J = 16.6$ Hz), 7.20 (t, 1H, $J = 7.8$ Hz), 7.25–7.30 (m, 2H), 7.38 (t, 2H, $J = 7.6$ Hz), 7.54 (d, 2H, $J = 7.6$ Hz), 7.61 (d, 1H, $J = 7.8$ Hz), 7.65 (d, 1H, $J = 7.8$ Hz), 7.74 (d, 1H, $J = 16.6$ Hz); $^{13}\text{C-NMR}$ (CDCl_3 , ppm) δ 25.95, 61.65, 124.59, 125.96, 126.06, 126.48, 126.82, 127.30, 127.32, 127.47, 128.70, 134.28, 138.10, 147.63; MS (m/z) 267 (M^+), calcd for $M = 267.36$.

***m*-Stilbene-*N*-*tert*-butylhydroxylamine**: yield 11%; mp 156 °C; IR (KBr pellet, cm^{-1}) 3221 (ν *o*-H), 964 (δ *trans*-HC=CH); $^1\text{H-NMR}$ (CDCl_3 , 500 MHz; ppm) δ 1.15 (s, 9H), 7.06 (s, 2H), 7.08 (s, 1H), 7.13 (d, 1H, $J = 7.8$ Hz), 7.21 (t, 1H, $J = 7.8$ Hz), 7.24–7.27 (m, 2H), 7.35 (t, 2H, $J = 7.6$ Hz), 7.37 (s, 1H), 7.51 (d, 2H, $J = 7.6$ Hz); $^{13}\text{C-NMR}$ (CDCl_3 , ppm) δ 25.96, 60.64, 122.67, 123.36, 124.03, 126.48, 127.54, 127.71, 128.58, 128.64, 128.76, 136.81, 137.32, 149.62; MS (m/z) 267 (M^+), calcd for $M = 267.36$. Anal. Calcd for $\text{C}_{18}\text{H}_{21}\text{NO}$: C, 80.9; H, 7.9; N, 5.2. Found: C, 80.6; H, 8.0; N, 4.9.

These hydroxylamines were treated with Ag_2O in degassed benzene solution to give the corresponding radicals, using the procedure described above for the bis(nitroxides). The same oxidation could be carried out in toluene, but the results were less satisfactory.

Acknowledgment. This work was partially supported by a Grant-in-Aid for Scientific Research on Priority Area "Molecular Magnetism" (Area No. 228/04242104) and for Scientific Research (No. 040852) from the Ministry of Education, Science and Culture, Japan. P.M.L. acknowledges support from the National Science Foundation (CHE 9204695). N.Y. acknowledges financial support from the Japan Society for the Promotion of Science (JSPS) for a research fellowship at the University of Massachusetts, Amherst.